

SEA-ICE DRAFT AND VELOCITIES FROM MOORINGS ON THE LABRADOR SHELF (MAKKOVIK BANK): 2003-2011

I.K. Peterson, S.J. Prinsenbergh and D. Belliveau

Ocean and Ecosystem Sciences Division
Maritimes Region
Fisheries and Oceans Canada

Bedford Institute of Oceanography
P.O. Box 1006
Dartmouth, Nova Scotia
Canada B2Y 4A2

2013

**Canadian Technical Report of
Hydrography and Ocean Sciences 281**

Canadian Technical Report of Hydrography and Ocean Sciences

Technical reports contain scientific and technical information of a type that represents a contribution to existing knowledge but which is not normally found in the primary literature. The subject matter is generally related to programs and interests of the Oceans and Science sectors of Fisheries and Oceans Canada.

Technical reports may be cited as full publications. The correct citation appears above the abstract of each report. Each report is abstracted in the data base *Aquatic Sciences and Fisheries Abstracts*.

Technical reports are produced regionally but are numbered nationally. Requests for individual reports will be filled by the issuing establishment listed on the front cover and title page.

Regional and headquarters establishments of Ocean Science and Surveys ceased publication of their various report series as of December 1981. A complete listing of these publications and the last number issued under each title are published in the *Canadian Journal of Fisheries and Aquatic Sciences*, Volume 38: Index to Publications 1981. The current series began with Report Number 1 in January 1982.

Rapport technique canadien sur l'hydrographie et les sciences océaniques

Les rapports techniques contiennent des renseignements scientifiques et techniques qui constituent une contribution aux connaissances actuelles mais que l'on ne trouve pas normalement dans les revues scientifiques. Le sujet est généralement rattaché aux programmes et intérêts des secteurs des Océans et des Sciences de Pêches et Océans Canada.

Les rapports techniques peuvent être cités comme des publications à part entière. Le titre exact figure au-dessus du résumé de chaque rapport. Les rapports techniques sont résumés dans la base de données *Résumés des sciences aquatiques et halieutiques*.

Les rapports techniques sont produits à l'échelon régional, mais numérotés à l'échelon national. Les demandes de rapports seront satisfaites par l'établissement auteur dont le nom figure sur la couverture et la page de titre.

Les établissements de l'ancien secteur des Sciences et Levés océaniques dans les régions et à l'administration centrale ont cessé de publier leurs diverses séries de rapports en décembre 1981. Vous trouverez dans l'index des publications du volume 38 du *Journal canadien des sciences halieutiques et aquatiques*, la liste de ces publications ainsi que le dernier numéro paru dans chaque catégorie. La nouvelle série a commencé avec la publication du rapport numéro 1 en janvier 1982.

**Canadian Technical Report of
Hydrography and Ocean Sciences 281**

2013

**SEA-ICE DRAFT AND VELOCITIES FROM MOORINGS ON THE LABRADOR
SHELF (MAKKOVIK BANK): 2003-2011**

by

I.K. Peterson, S.J. Prinsenber and D. Belliveau

**Ocean and Ecosystem Sciences Division
Maritimes Region
Fisheries and Oceans Canada**

**Bedford Institute of Oceanography
P.O. Box 1006
Dartmouth, Nova Scotia
Canada, B2Y 4A2**

© Her Majesty the Queen in Right of Canada, 2013.
Cat. No. Fs97-18/281 E ISSN:1488-5417

Correct Citation for this publication:

Peterson, I.K., S.J. Prinsenberg and D. Belliveau. 2013. Sea-Ice Draft and Velocities from Moorings on the Labrador Shelf (Makkovik Bank): 2003-2011. Can. Tech. Rep. Hydrogr. Ocean Sci. 281: v + 32 p.

TABLE OF CONTENTS

ABSTRACT	iv
RÉSUMÉ	v
1.0 INTRODUCTION	1
2.0 INSTRUMENTATION	2
3.0 MAXIMUM AND MEAN DAILY ICE DRAFT	2
4.0 DAILY ICE DRAFT DISTRIBUTIONS	5
5.0 ICE CHARTS	16
6.0 DAILY ICE AND WIND VELOCITIES	19
7.0 WIND EFFECTS ON ICE DRAFT	22
8.0 WATER BOTTOM TEMPERATURES	22
9.0 ENVISAT AND RADARSAT-2 SAR DATA	23
10.0 CONCLUSIONS	30
11.0 ACKNOWLEDGMENTS	31
12.0 REFERENCES	31

ABSTRACT

Peterson, I.K., S.J. Prinsenberg and D. Belliveau. 2013. Sea-Ice Draft and Velocities from Moorings on the Labrador Shelf (Makkovik Bank): 2003-2011. Can. Tech. Rep. Hydrogr. Ocean Sci. 281: v + 32 p.

Sea ice draft over the Labrador Shelf was measured using an upward-looking ice profiling sonar (IPS) moored on Makkovik Bank every second year for the ice seasons of 2002-2003, 2004-2005, 2006-2007, 2008-2009 and 2010-2011. The temporal data were converted to a spatial series using ice velocity data collected with an acoustic Doppler current profiler (ADCP), and were compared with ice signatures in ENVISAT and RADARSAT-2 synthetic aperture radar (SAR) imagery, surface wind data from the CMC (Canadian Meteorological Centre) regional model, and ice charts from the Canadian Ice Service.

The maximum ice drafts were 22, 16, 21, 21 and 21m, and the mean daily ice drafts were 2.2, 1.3, 2.8, 2.5 and 1.1m in 2003, 2005, 2007, 2009 and 2011 respectively. In the three heavy ice years (2003, 2007 and 2009), there appeared to be a breakdown of the deformed ice (ridges) near the onset of the melt season, when the air temperature rose above 0°C. Ice volume inferred from the ice draft data is about twice the volume estimated from Canadian Ice Service ice charts which depict undeformed ice only, however the ratio is highly variable because of variability in ice deformation. Daily mean ice velocities were 1.8-2.9% of the surface (10m) wind speed, and 17-41° to the right of the wind. The surface wind explains 56-72% of the variance in ice velocity. Ice signatures inferred from SAR imagery were consistent with the ice draft data.

RÉSUMÉ

Peterson, I.K., S.J. Prinsenberg and D. Belliveau. 2013. Sea-Ice Draft and Velocities from Moorings on the Labrador Shelf (Makkovik Bank): 2003-2011. Can. Tech. Rep. Hydrogr. Ocean Sci. 281: v + 32 p.

Le tirant d'eau glacial de la mer dans le plateau du Labrador a été mesuré à l'aide d'un sonar profileur de glace à vision vers le haut, amarré au banc Makkovik tous les deux ans pour les saisons des glaces de 2002-2003, de 2004-2005, de 2006-2007, de 2008-2009 et de 2010-2011. Les données temporelles ont alors été converties en séries spatiales en utilisant les données de vitesse des glaces recueillies à l'aide d'un profileur de courant à effet Doppler, puis elles ont été comparées aux signatures des glaces provenant des images du radar à synthèse d'ouverture d'ENVISAT et de RADARSAT-2, aux données de vents de surface provenant du modèle régional du Centre météorologique canadien ainsi qu'aux cartes des glaces provenant du Service canadien des glaces.

Les tirants d'eau glacial maximums étaient de 22 m, de 16 m, de 21 m, de 21 m et de 21 m, et la moyenne des tirants d'eau glacial quotidiens étaient de 2,2 m, de 1,3 m, de 2,8 m, de 2,5 m et de 1,1 m en 2003, en 2005, en 2007, en 2009 et en 2011 respectivement. Durant les trois années de forte glace (2003, 2007 et 2009), il semblait y avoir une détérioration de la glace déformée (crêtes) vers le début de la saison de la fonte lorsque la température de l'air dépassait 0 °C. Le volume de glace déduit des données des tirants d'eau glacial est environ le double du volume estimé à partir des cartes des glaces du Service canadien des glaces qui n'indiquent que de la glace non déformée. Toutefois, le ratio varie considérablement en raison de la variabilité de la déformation de la glace. Les vitesses moyennes des glaces quotidiennes représentaient de 1,8 à 2,9 % de la vitesse du vent de surface (10 m), et se déplaçaient de 17 à 41° à droite de la direction du vent. Le vent de surface explique l'écart de 56 à 72 % dans la vitesse des glaces. Les signatures des glaces déduites des images du radar à synthèse d'ouverture étaient semblables aux données des tirants d'eau glacial.

1.0 INTRODUCTION

Beginning in December 2002, moorings were deployed by personnel of the Bedford Institute of Oceanography on Makkovik Bank, on the central Labrador Shelf every second year to monitor sea ice draft, ice velocity and ocean currents. The aim of the project was to fill an environmental data gap, in order to enhance the safety and efficiency of offshore oil and gas exploration and offshore operations (shipping), to provide data for offshore platform design, and to serve as a validation data set for numerical ice-ocean models. Sea ice draft data were collected with an Ice Profiling Sonar (IPS), or upward-looking sonar (ULS), and ice velocity and ocean current data were collected with an Acoustic Doppler Current Profiler (ADCP) moored nearby. The ice velocity data were used to convert the sea ice draft time series to spatial series, in order to derive ice draft histograms and ice keel statistics (Ross et al., 2006). Water temperature and conductivity were measured with a MicroCat recorder moored beneath the upward-looking sonar near the bottom of the water column.

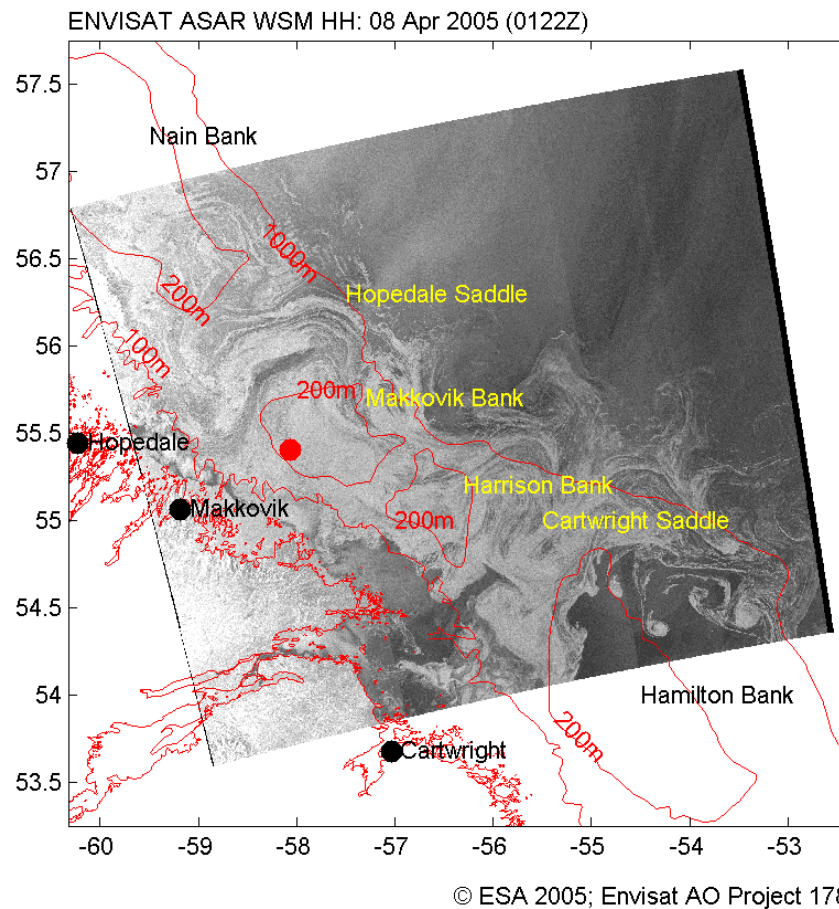


Figure 1. Envisat SAR image showing sea ice over the Labrador Shelf in the vicinity of the mooring site on Makkovik Bank (red dot).

The mooring site was on the western side of Makkovik Bank (Fig. 1), where the water depth is approximately 100m. The SAR image in Fig. 1 shows features of the general circulation in the area as inferred from ice stream patterns. There is an eastward flow through Hopedale Saddle north of Makkovik Bank, and undulations in the Labrador Current propagate southward near the shelf break (LeBlond, 1982).

2.0 INSTRUMENTATION

The Ice Profiling Sonar (IPS) used to measure ice draft was manufactured by ASL Environmental Sciences Inc., and has been used extensively in the Beaufort Sea for many years (Melling and Riedel, 1996). An SBE-SM MicroCAT C-T (conductivity-temperature) recorder, manufactured by Seabird Electronics, Inc., which also measured pressure, was moored beneath the IPS near the ocean bottom for estimating sound speed, which is used in the processing of ice draft data. An Acoustic Doppler Current Profiler (ADCP) manufactured by RD Instruments was used to measure ice drift and ocean currents. Data quality was enhanced using streamlined buoyancy packages which reduce mooring drag and motion (Hamilton et al., 2002). The IPS is best positioned at a depth of 30-100m, and has a field of view of approximately 0.8m from a depth of 50m (Melling and Riedel, 2004). The velocity components are averaged over a period of approximately 5 minutes once per hour. Processing of the ice draft data (time series and spatial series) was done by ASL Environmental Sciences Inc. (Ross et al., 2006). The ice draft time series data are provided at 2-second intervals, while the spatial series are provided at 1 m intervals. Because the ADCP deployed in 2011 was lost, only time series data are available for that year.

3.0 MAXIMUM AND MEAN DAILY ICE DRAFT

Daily maximum and mean ice drafts (Fig. 2, Table 1) were computed from the spatial series of ice draft in 2003, 2005, 2007 and 2009, and from the time series data in 2011. Gaps in the data generally represent periods when the ice edge was north or west of the mooring site. In 2003, ice appeared in mid-January and lasted until early June. In 2005, ice appeared in early January and disappeared in mid-May, and in 2007, ice appeared in late January and lasted until late June. In 2009, ice appeared in mid-January and disappeared in mid-June, and in 2011, ice appeared in early February and disappeared in mid-May. In all 5 years, the maximum ice draft occurred in April, and ranged from 16 to 22m.

Table 1. Maximum and mean daily sea ice draft (from spatial ice draft series) and ice drift from ADCPs. Deep feature events are also listed.

	2003	2005	2007	2009	2011
Maximum Sea Ice Draft (m)	22.4 (02 Apr)	15.9 (05 Apr)	21.1 (30 Apr)	21.0 (16 Apr)	20.9 (28 Apr)
Mean Daily Sea Ice Draft (m)	2.2	1.3	2.8	2.5	1.1
Maximum Ice Speed (cm/s)	89.5	90.4	89.8	113.4	
Mean Ice Speed (cm/s)	26.3	28.7	21.7	20.9	
Depth (m) (Date of Deep Features)	>46.8 (19 May)		50.5 (19 May) 37.1 (20 May) 69.7 (18 Jun)	47.7 (26 Feb) 47.2 (28 Feb) 60.1 (10 Mar) 40.0 (15 Apr)	57.2 (22 May) 32.6 (30 May)

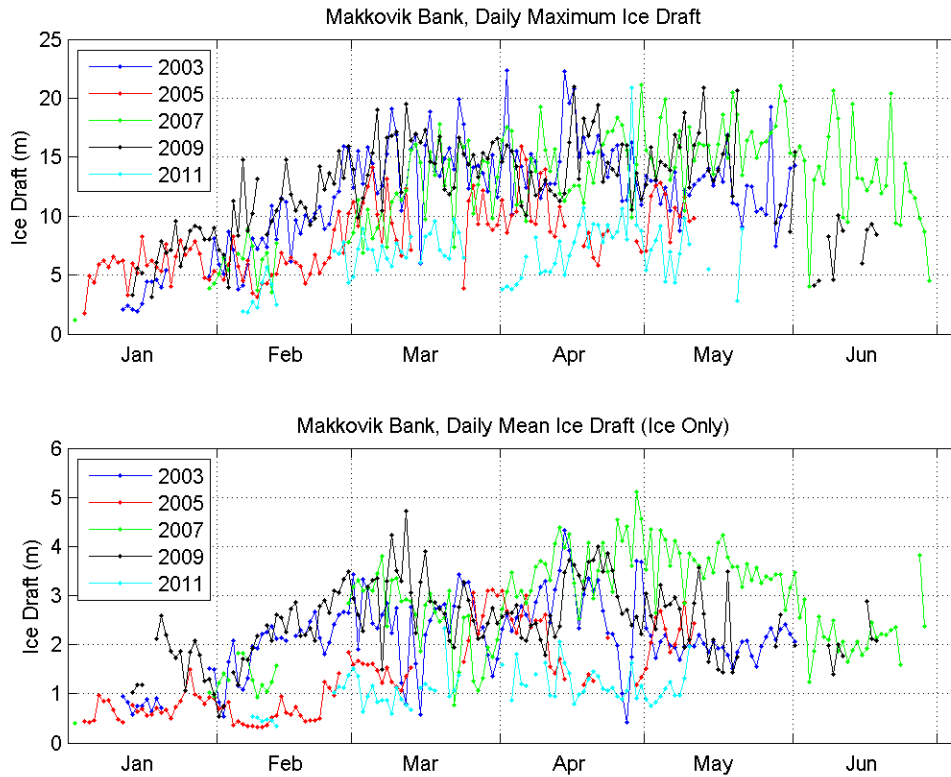


Figure 2. Maximum and mean daily ice draft in 2003-2011.

For the years 2003-2009, daily mean ice draft increases through the ice season from the date of appearance until April when it reaches 3-5m, and starts declining in May. Near the end of the ice season, the daily mean draft remains relatively constant at about 2m until breakup. However in 2011, mean ice draft remained low at about 1-2m after early March. The mean ice draft was relatively high in 2003, 2007 and 2009 (2.2m, 2.8m, and 2.5m) and low in 2005 and 2011 (1.3m and 1.1m). The plots show that the ice seasons of 2005 and 2011 were the least severe and that of 2007 lasted the longest. The light ice conditions in 2011 relative to 2009 are consistent with ice thickness measurements obtained with a helicopter-borne electromagnetic system in those years (Prinsenberget al., 2011, 2012).

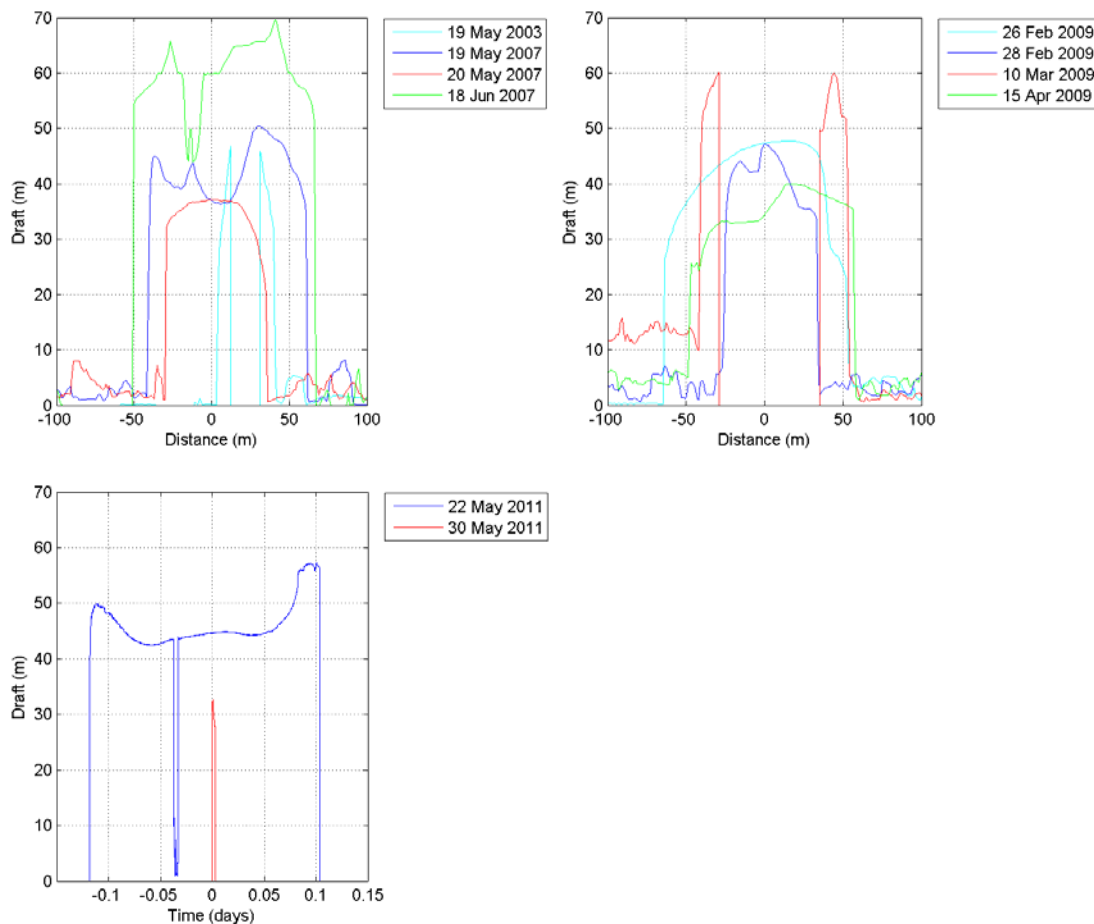


Figure 3. Deep ice features (>30m draft).

In Fig. 2 which is meant to represent sea ice only, the data from several deep ice features with drafts of over 30m have been removed. The number of deep ice features removed was one in 2003, three in 2007, four in 2009 and two in 2011 (Fig. 3). After a deep feature of over 47m was observed in 2003, the blanking period was adjusted to provide higher ice drafts in subsequent years. Deep features of 37m, 51m and 70m were observed in 2007, 40, 47, 48 and >60m in

2009, and 33m and 57m in 2011. As suggested by Ross et al. (2003), the deep ice features are likely icebergs or bergy bits rather than sea ice. The deeper feature in 2011 (57 m) was over the mooring for over 5 hours. It corresponds to the Petermann ice island PII-Bb, which was part of the large calving event of the Petermann glacier in northwestern Greenland in the summer of 2010.

4.0 DAILY ICE DRAFT DISTRIBUTIONS

Daily ice draft distributions in the five deployment years are plotted in the upper panels of Figures 4a-e. For each vertical line, the plot shows the ice draft distribution observed for that day in terms of the probability density function following Wadhams et al. (1985). The colour code shows the proportion of the ice on each day within a given ice draft bin divided by the bin size (10 cm), i.e. the proportions integrated over the full range of draft equal one. The mean ice draft (black line), the maximum ice draft divided by 4 (pink line), and the ice concentration (red line) are also plotted. In all five years, there is relatively low variance in ice thickness at the beginning of the ice season. By April in all years except 2011, there are larger fractions of ice thicker than 3m, which represents deformed or old ice. At the end of the ice season, there is a better defined peak in ice thickness at about 1-1.5m, which represents level medium to thick first year ice.

The modal ice draft is the most commonly observed ice draft, i.e. it corresponds to the draft with the highest value in the ice draft distribution. It can be seen that the modal ice draft is nearly equal to the mean in the early winter, but is lower than the mean in the spring when the draft distribution is skewed due ice ridges. In general, there was less deformed ice in 2005 and 2011 than in the other 3 years.

Figure 5 shows 10m wind velocities and 2m air temperatures from the CMC (Canadian Meteorological Centre) regional model (2003-2009) interpolated to the mooring position, and surface wind velocities and air temperatures from the NCEP/NCAR Reanalysis 1 dataset (Kalnay et al., 1996) in 2011. (CMC data are available for 2011 also, but were not used since the ADCP was not recovered in 2011, and a detailed comparison with wind data was not possible). It can be seen that the transition from deformed to predominantly level ice near the end of the ice season, is at about the same time that air temperatures rise above 0°C.

Thus it appears that there is a breakdown of ridges and rubble occurring around the onset of the melt season. Such a breakdown of ridges was observed in the Antarctic region by Steer et al. (2008), who suggested that ridges relax and break into their component parts due to ice melt and divergence of the pack ice. When the air temperature rises above 0°C, the “glue” holding the ridge blocks together breaks down. In addition, the ice concentration decreases, allowing the ridges to “relax” into their component parts. Decreasing ice concentration would also

permit the penetration of ocean swell, which could also contribute to ridge breakdown.

The degree-days accumulated since 01 December at Cartwright, Labrador are shown in Fig. 6. For each day in 2003, 2005, 2007, 2009 and 2011 these were computed as the cumulative sum of daily mean air temperatures since 01 December, relative to 0°C. A positive slope in the degree-day curve denotes the time when the air temperature rises above 0°C. This occurred in late April in 2003, mid-April in 2005, early May in 2007, late April in 2009 and late April in 2011 (Table 2). In comparison, the ridges appeared to break down in late April, mid-April, mid-May, and mid-May in 2003, 2005, 2007, 2009 respectively, with little ridging in 2011. The dates when the ice concentration at the mooring site decreases rapidly from near 100% also showed a somewhat similar pattern: late April in 2003, early April in 2005, early June in 2007, mid-May in 2009 and late March in 2011. Thus in 2007 ridge collapse occurs two weeks before ice concentration decreases, and suggests that ice melt is more important than ice divergence to ridge collapse. However in other years, ridge collapse could be due to either ice melt or ice divergence.

Table 2. Times of melt onset (when air temperature rises above 0°C), ridge collapse and ice cover decrease.

	Melt onset	Ridge collapse	Ice cover decrease
2003	Late April	Late April	Late April
2005	Mid-April	Mid-April	Early April
2007	Early May	Mid-May	Early June
2009	Late April	Mid-May	Mid-May
2011	Late April	n/a	Late March

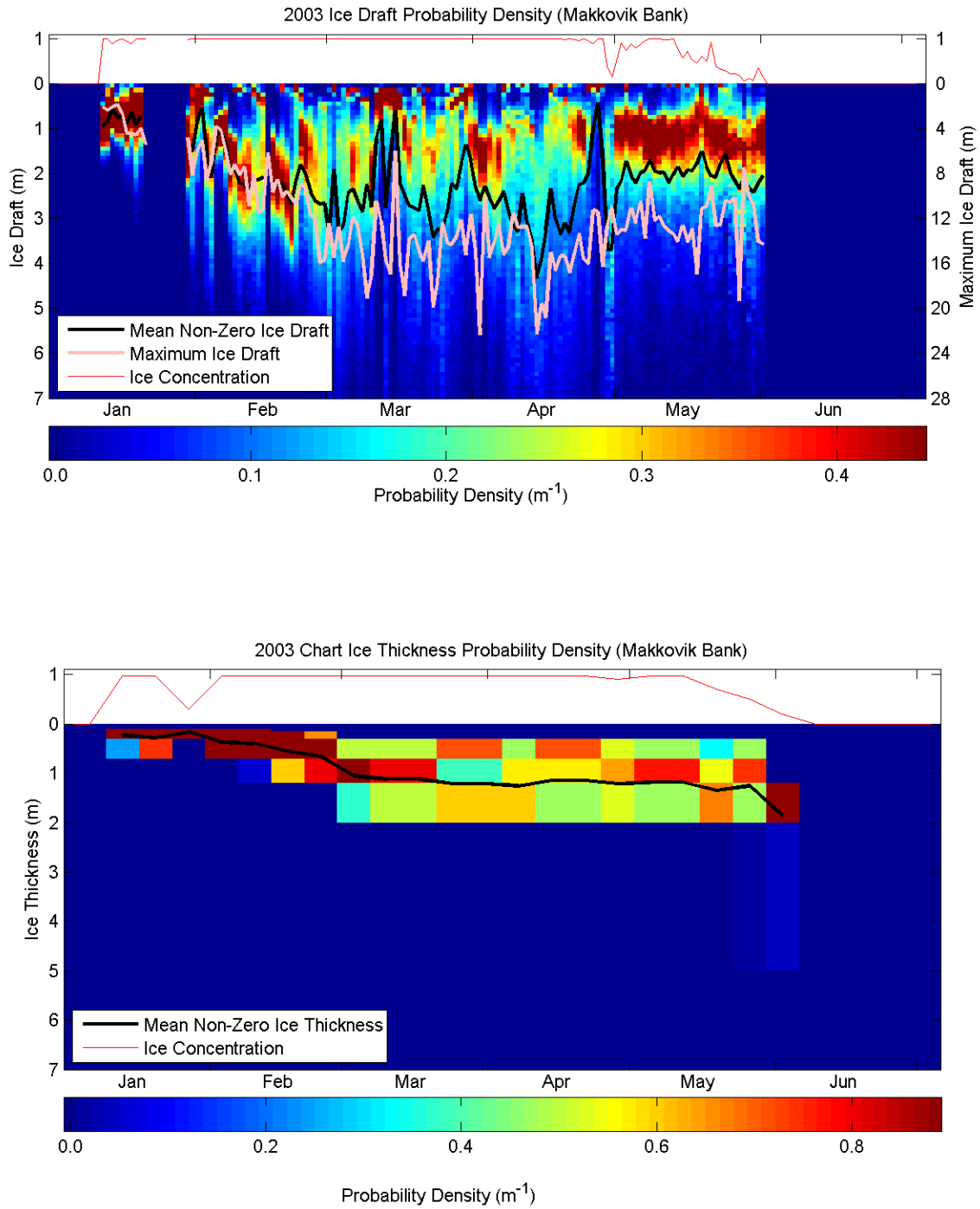


Figure 4a. Daily ice draft distribution from mooring (top) and ice thickness distributions from ice charts (bottom) in 2003.

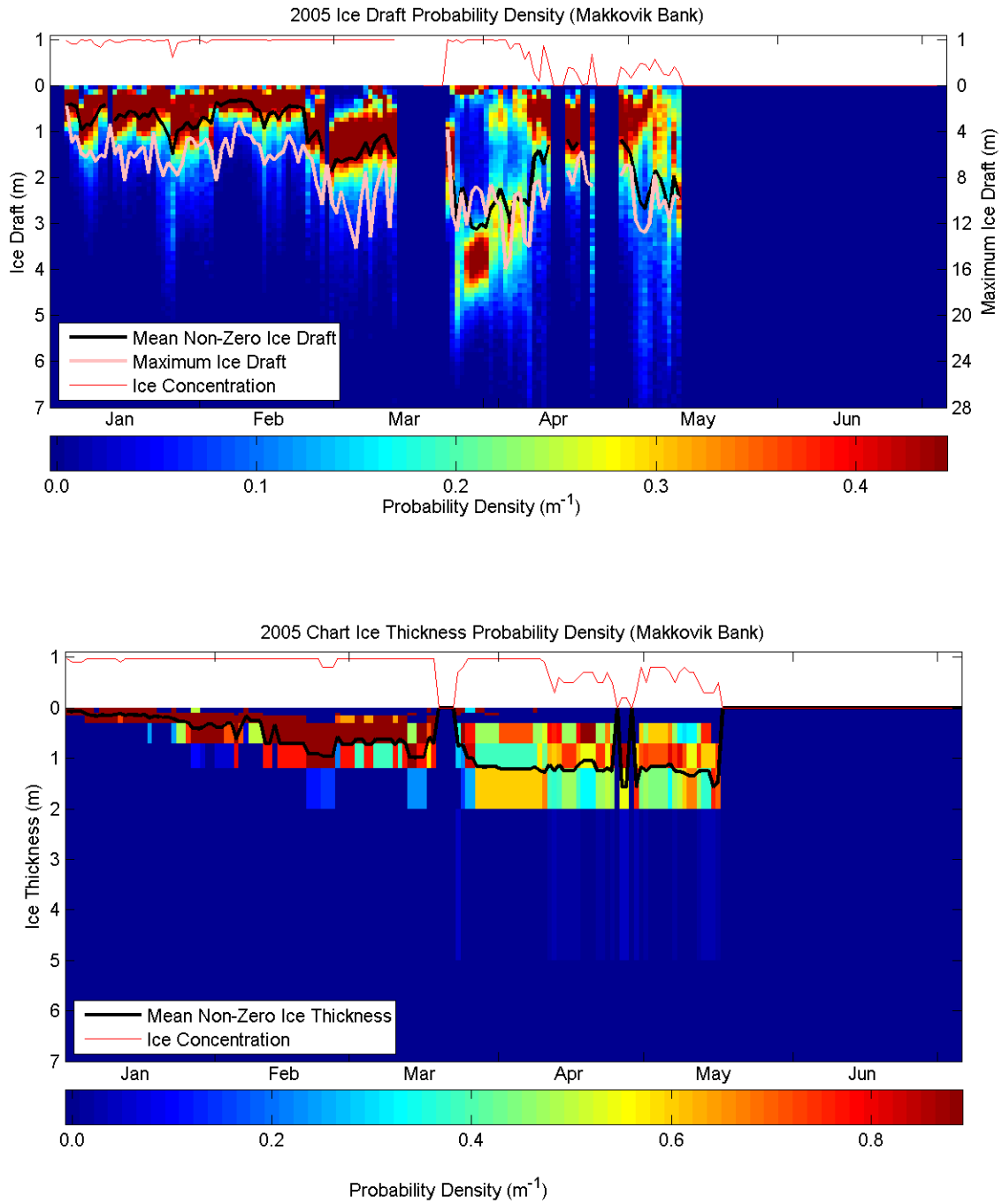


Figure 4b. Daily ice draft distribution from mooring (top) and ice thickness distributions from ice charts (bottom) in 2005.

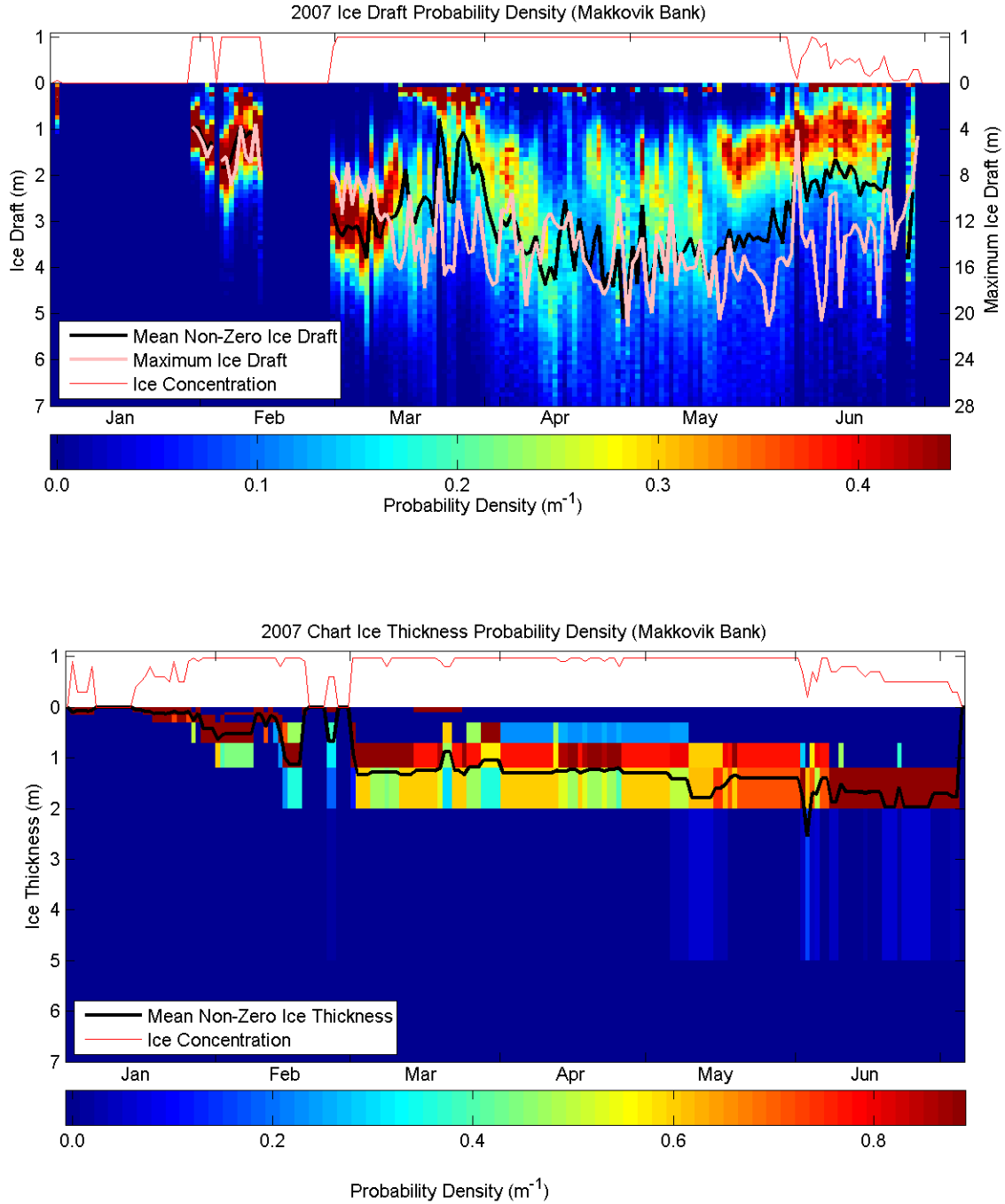


Figure 4c. Daily ice draft distribution from mooring (top) and ice thickness distributions from ice charts (bottom) in 2007.

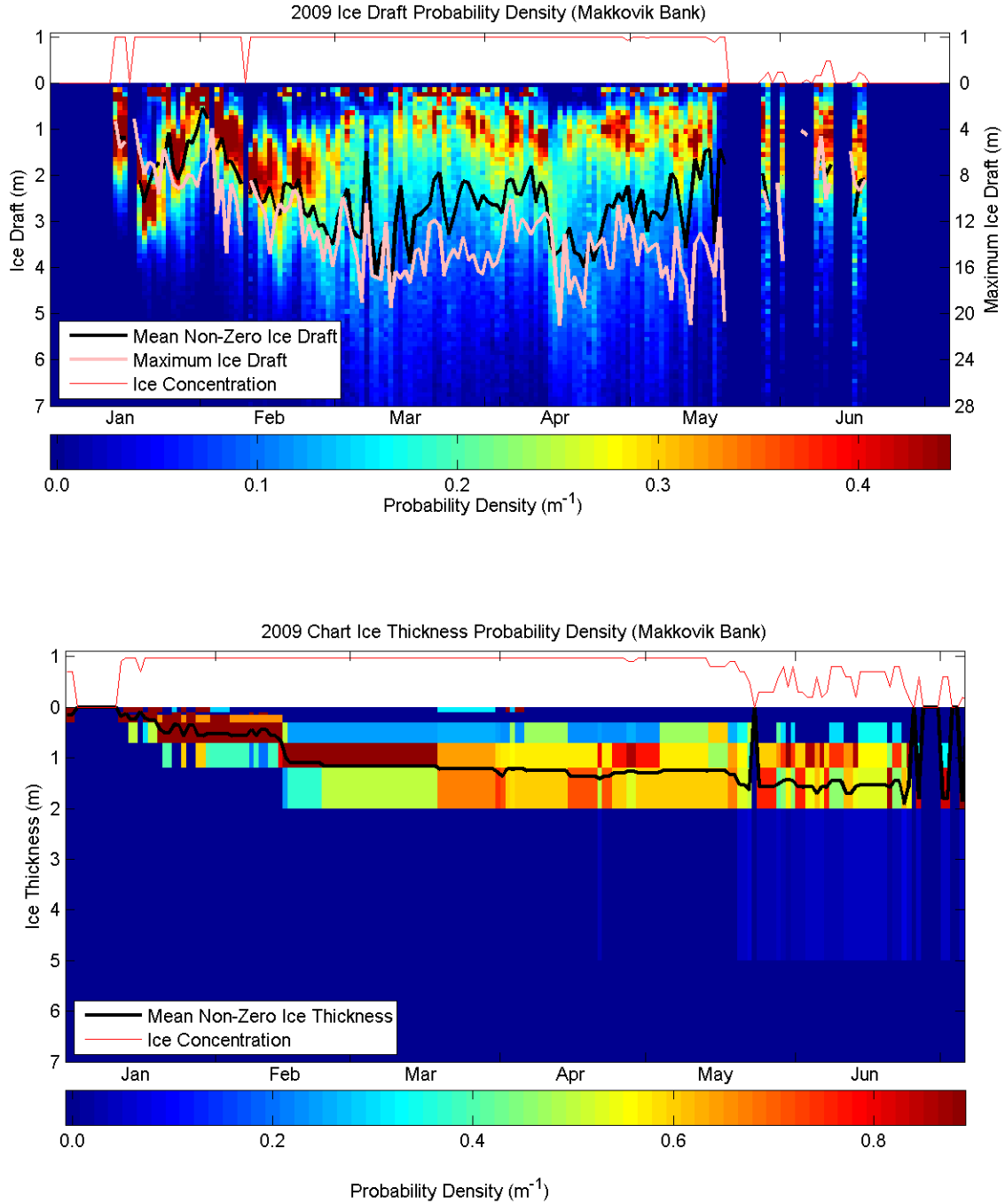


Figure 4d. Daily ice draft distribution from mooring (top) and ice thickness distributions from ice charts (bottom) in 2009.

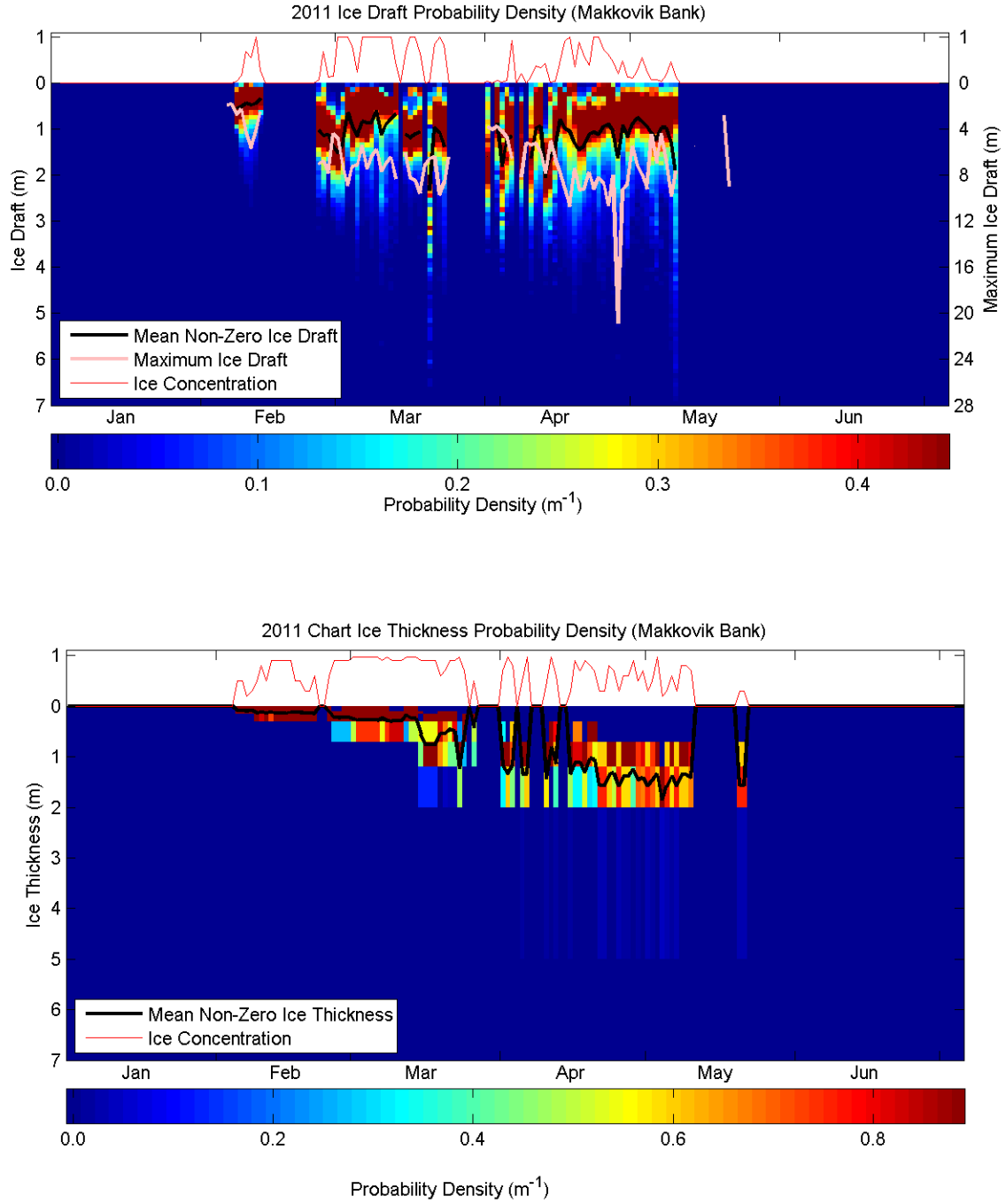


Figure 4e. Daily ice draft distribution from mooring (top) and ice thickness distributions from ice charts (bottom) in 2011.

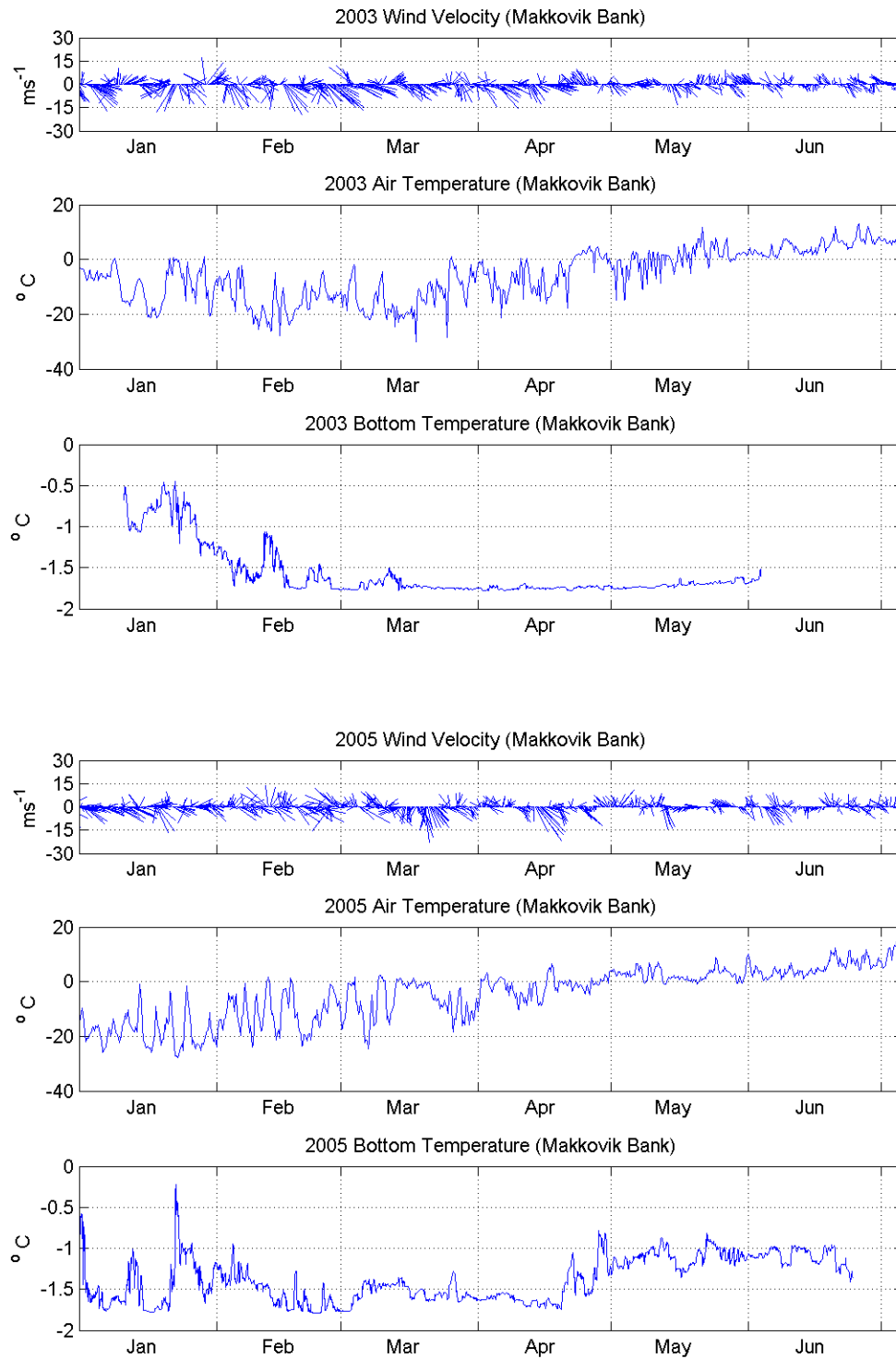


Figure 5. Wind velocity (10m) and air temperature (2m) from CMC regional model (2003-2009), and surface wind velocity and air temperature from the NCEP/NCAR Reanalysis 1 dataset (2011), and water bottom temperatures.

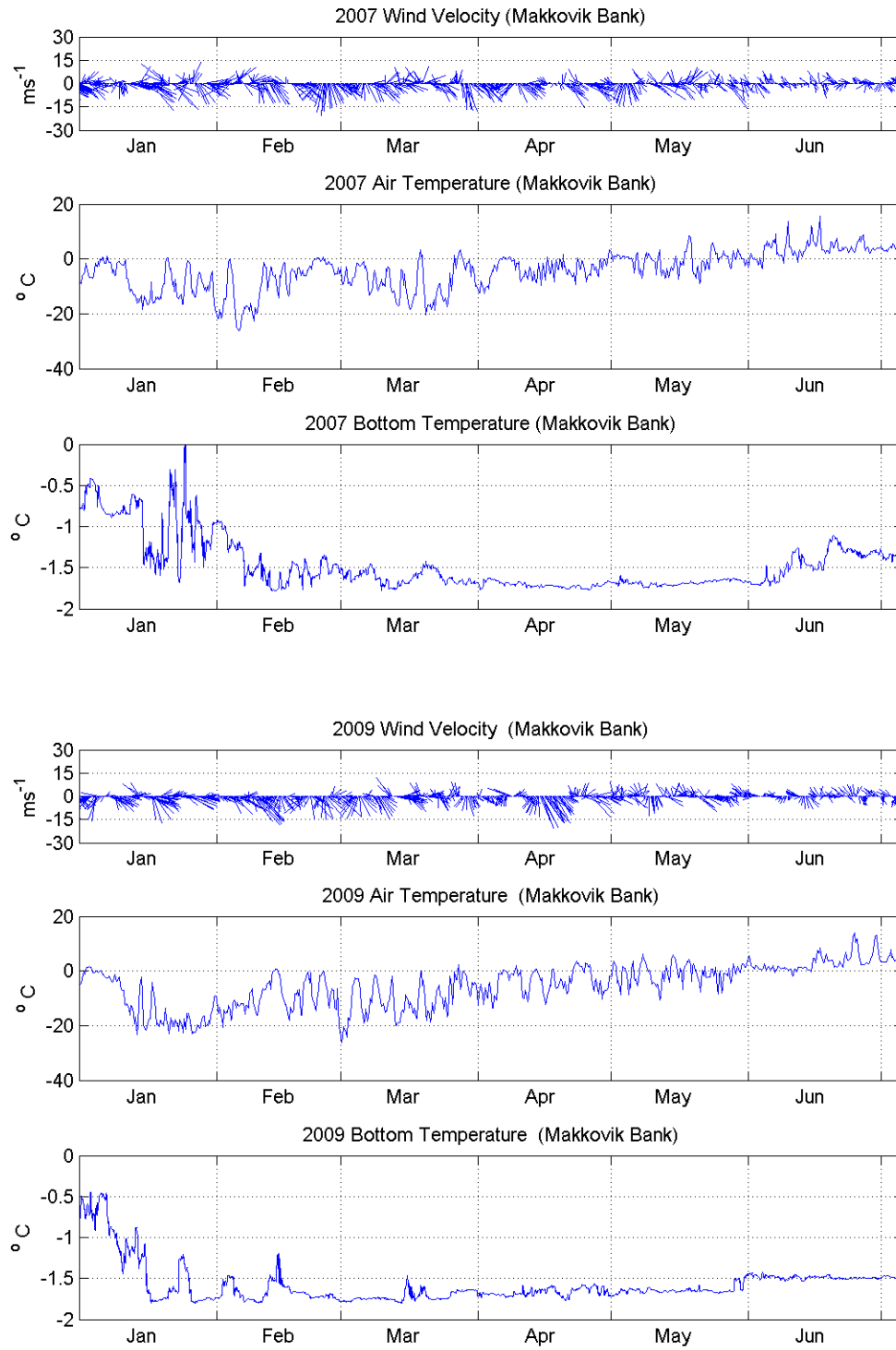


Figure 5 (cont).

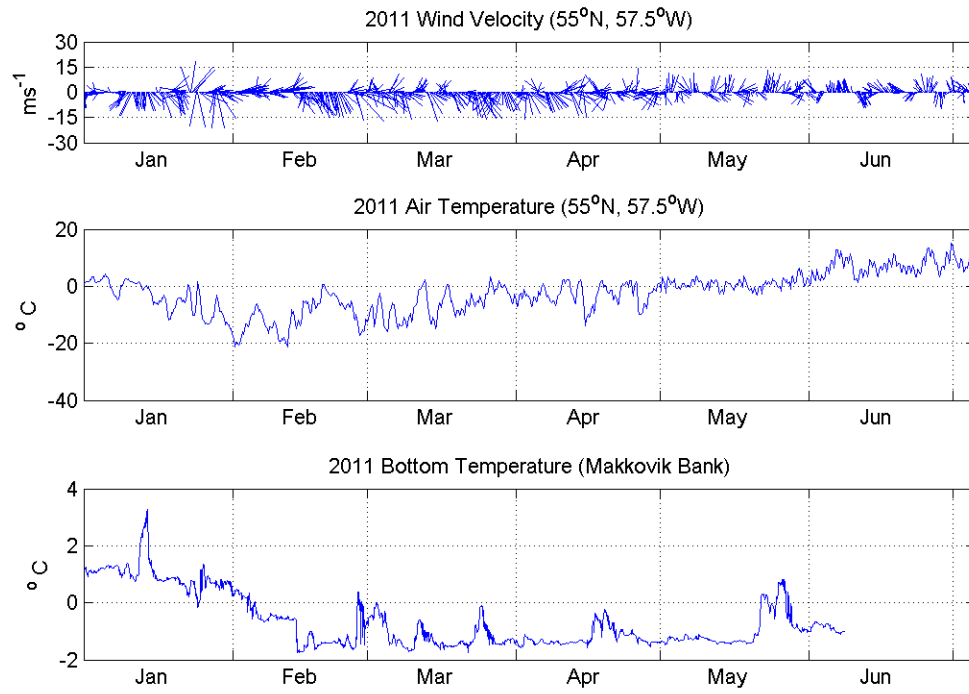


Figure 5 (cont.)

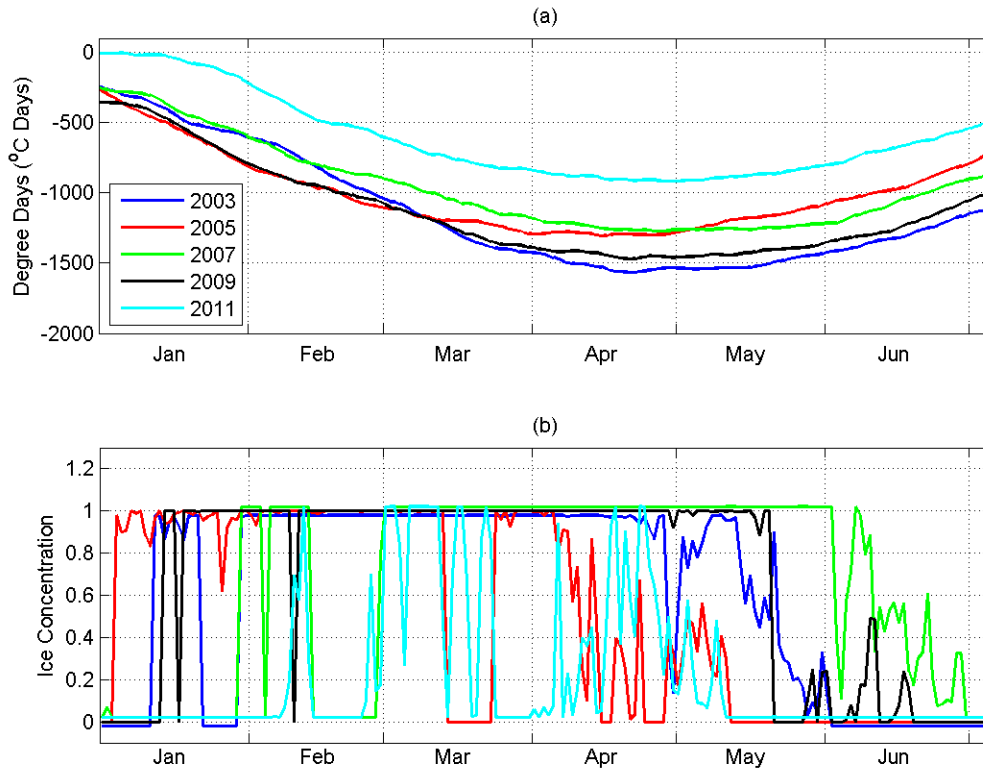


Fig. 6. (a) Degree-days relative to 0°C for 2003, 2005, 2007, 2009 and 2011 starting on 01 Dec, and (b) ice concentrations from mooring data.

Monthly mean air temperatures at Hopedale, NL for the 5 ice seasons are shown in Table 3. Temperatures are anomalously high in March-April 2005, and December-January 2011, in agreement with the light ice conditions observed in the early 2011 and late 2005 ice seasons (Fig. 6). Eastward winds were also low in December-January 2011 and March-April 2005 as expected, since offshore winds would result in more ice formation and less convergence.

Table 3. Monthly mean air temperature at Hopedale, NL (°C) measured by Environment Canada and the eastward wind component at 55°N, 60°W from the NCEP/NCAR Reanalysis 1 dataset.

	2002-2003	2004-2005	2006-2007	2008-2009	2010-2011
Air Temperature (°C)					
December	-10.9	-11.4	-8.8	-14.2	-2.0
January	-13.3	-21.0	-12.2	-15.8	-8.4
February	-18.1	-12.8	-11.4	-13.7	-16.8
March	-16.2	-9.3	-11.6	-13.2	-11.1
April	-6.2	-1.7	-5.4	-5.5	-6.1
Eastward Wind Component (m/s)					
December	4.4	5.0	7.7	6.6	0.4
January	4.0	6.5	5.1	6.5	3.0
February	5.3	3.1	3.5	4.0	7.0
March	5.4	1.5	4.7	3.5	3.8
April	3.5	2.2	2.5	2.6	3.5

5.0 ICE CHARTS

In Figure 4, the lower panels show the ice thickness distributions, mean ice thicknesses and ice concentrations at the mooring site given on ice charts produced by the Canadian Ice Service. The thicknesses assumed for the various ice types on the ice charts are shown in Table 4, along with the minimum and maximum thicknesses used in Fig. 4. For new, grey, grey-white, thin first-year (FY) and medium FY ice, the thicknesses are the mid-points of the minimum and maximum values given by the Canadian Ice Service (Environment Canada, 2005). The thickness of thick FY ice is given by CIS as >1.2m and no thickness is given for old ice. However, Bernard Miville at CIS compiled a set of weights called the TISI index with thicknesses of 1.6m for thick first-year ice and 3.5m for old ice. The maximum thickness of thick FY ice used in Fig. 4 was assumed to be 2.0 m (since the minimum and mean values are 1.2m and 1.6m respectively). The minimum and maximum thicknesses of old ice were assumed to be 2.0m and 5.0m (since the mean value from the TISI index is 3.5m).

Table 4. Ice thicknesses assumed for ice types in CIS ice charts.

Ice type	Minimum thickness (m)	Maximum thickness (m)	Mean thickness (m)
New ice	0	0.1	0.05
Grey ice	0.1	0.15	0.125
Grey-white ice	0.15	0.3	0.225
Thin FY ice	0.3	0.7	0.5
Medium FY ice	0.7	1.2	0.95
Thick FY ice	1.2	2.0	1.6
Old ice	2.0	5.0	3.5

There is good agreement between the upward-looking sonar data and the ice chart data in the timing of major changes in the ice regime (Fig. 4). However, because the ice charts show level ice concentrations only, the mean ice thickness is lower for the ice chart data, even though freeboard height is included in the ice chart thicknesses but not the ice draft measurements.

Daily mean ice draft is compared to mean ice thickness from CIS ice charts in Fig. 7a, with the blue line representing a 1:1 ratio between ULS ice draft and chart ice thickness. There is a lot of scatter in the individual points (crosses) between years due mainly to varying amounts of deformed ice, with low ice drafts relative to ice chart thicknesses in 2005 and 2011 and high ice drafts in 2003, 2007 and 2009. The black dots (connected by black lines) represent the median ice thicknesses and ice drafts for the ice chart thickness ranges of 0-0.5m, 0.5-1m, 1-1.5m and 1.5-2m.

In general, the ratio of ice draft to chart ice thickness (Fig. 7b) decreases from 3.7 for chart ice thicknesses of 0-0.5m, to 2.4 for chart ice thicknesses of 0.5-1.0m, and 2.1 for chart ice thicknesses of 1.0-1.5m. For thicknesses greater than 1.5m, the mean draft remains constant at about 2.1m (Fig. 7a). The ratio of ice draft to chart ice thickness at low ice chart thicknesses is as high or higher than at high ice thicknesses. Thus deformation of thin ice due to rafting appears to be at least as important as ridging of thicker ice types, in affecting the true ice thickness. The overall mean ratio of ice draft to chart ice thickness is 2.4.

To include the freeboard contribution to the ice draft measurements and thus convert ice draft to ice thickness, the following relationship is used:
 $h/h_W = \rho_w/\rho_i$, where h is ice thickness, h_W is ice draft, ρ_w is water density, and ρ_i

is ice density. Assuming that $\rho_w = 1.027 \text{ Mg/m}^3$ and $\rho_i = 0.915 \text{ Mg/m}^3$, the ratio of ice thickness to ice draft is 1.1, and the ratio of inferred ice thickness from the ULS data to ice chart ice thickness becomes 2.6.

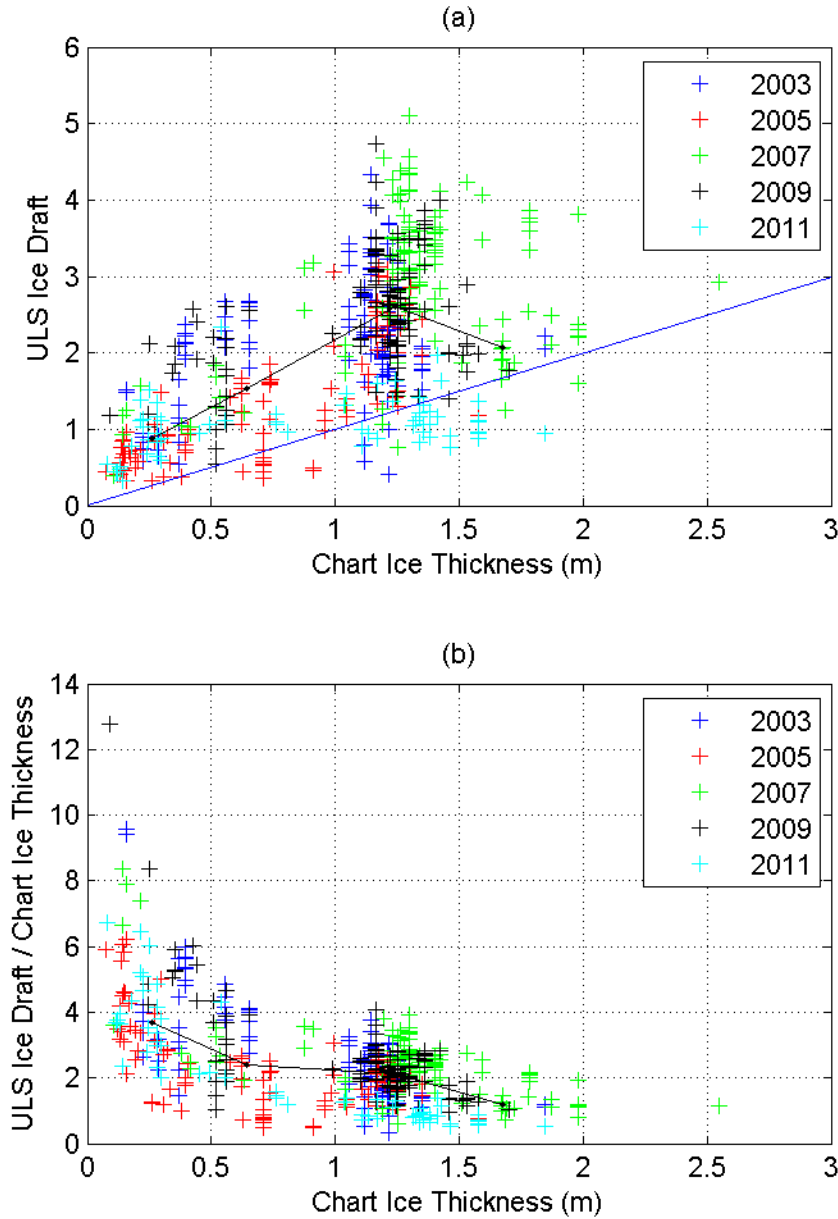


Fig. 7. (a) Daily mean ice draft from upward looking sonar (ULS) versus ice thickness from ice charts, and (b) ratio of ULS ice draft to ice thickness from CIS ice charts.

However, deformed ice is porous, i.e. it contains voids of seawater between the blocks, so the ice draft measurements have to be reduced to account for this in calculations of ice volume. The mean porosity of deformed ice is typically 0.2-0.3

(Marchenko, 2008), so assuming a mean porosity value of 0.25, the ratio of solid ice thickness to chart ice thickness is 2.0.

6.0 DAILY ICE AND WIND VELOCITIES

Daily maximum and mean hourly ice speeds measured with the ADCP in 2003-2009 are shown in Fig. 8 and Table 1. Maximum ice speeds are 90-113 cm/s and mean speeds are 21-29 cm/s. For 2003 and 2005, a high confidence velocity dataset (dots in Fig. 8) was also produced, with maximum speeds of about 77 cm/s (Ross et al., 2006).

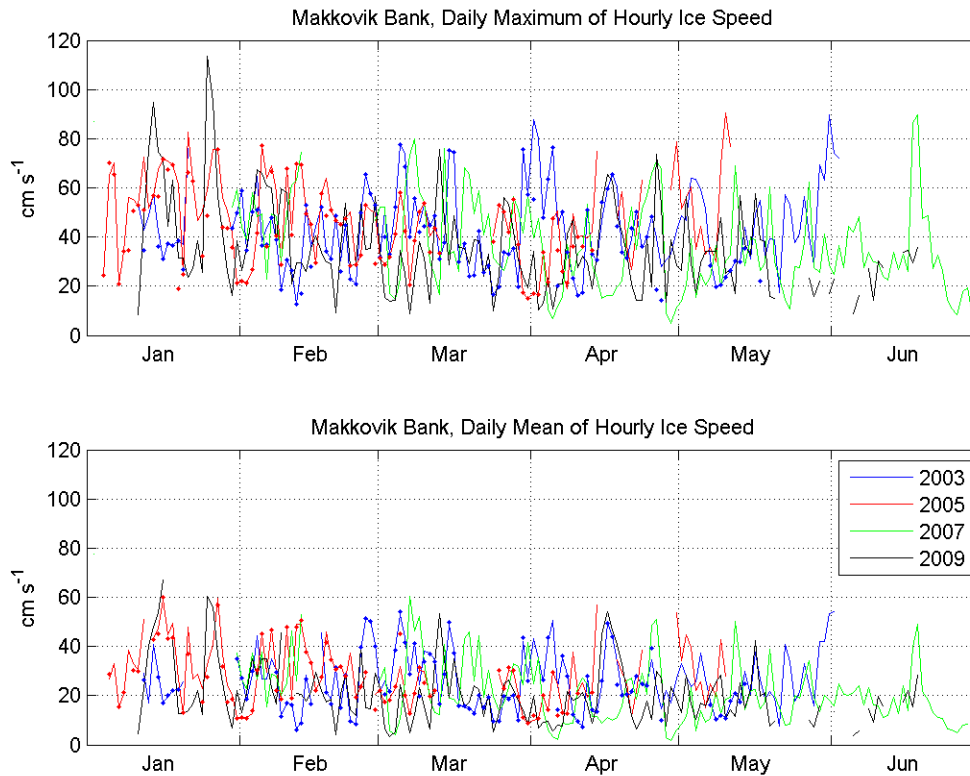


Figure 8. Daily maximum and mean ice speeds in 2003, 2005, 2007 and 2009. The dots represent values from the high confidence velocity datasets.

Ice velocities are plotted along with wind velocities from the CMC regional model, interpolated to the mooring site (Fig. 9). Table 5 shows the results of a complex regression analysis between ice velocity and wind velocity, using the regression model: $u_i = Ae^{-i\theta} u_w + C + \epsilon$, where u_i is the ice velocity, u_w is the wind velocity, A is the scaling factor, θ is the turning angle, C is the mean ocean current, and ϵ is the error, following Thorndike and Colony (1982).

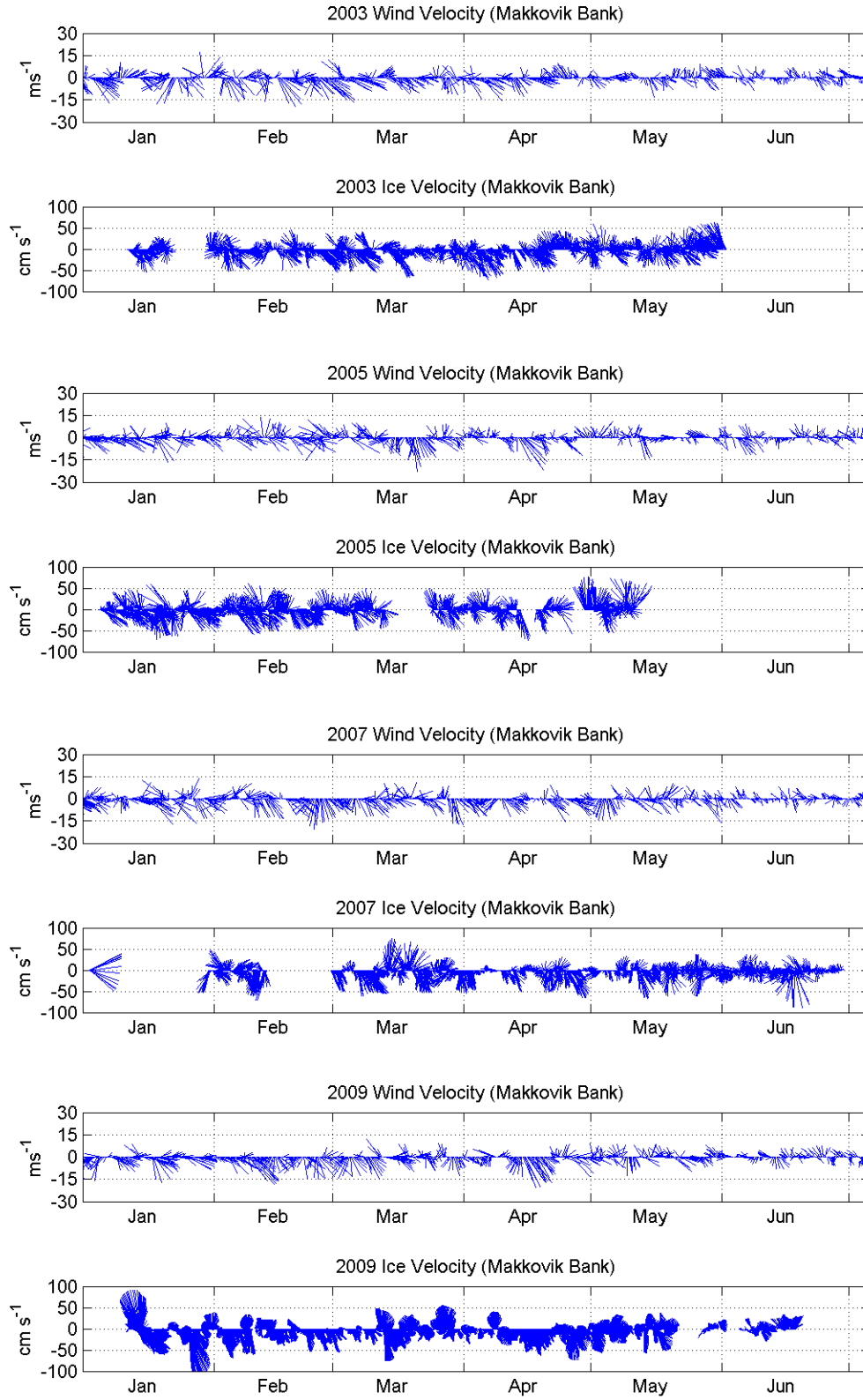


Fig. 9. Wind velocities from CMC regional model and ice velocities from ADCPs.

For the four years (2003, 2005, 2007 and 2009), the scaling factors are 1.8-2.9% of the wind speed, the turning angles are 17-41 degrees to the right of the wind, the root-mean-square error is 0.12-0.13 m/s, and the squared correlation coefficients are 0.56-0.72 ($p < 0.01$). The mean current term in all four years is less than 5 cm/s. In comparison, Thorndike and Colony (1982) reported turning angles in the Arctic of 5 and 18 degrees relative to geostrophic winds in winter and summer, or 35 and 43 degrees relative to 10m winds. They reported scaling factors of 0.77% and 1.05% relative to geostrophic winds in winter and summer, or 1.4% and 1.8% relative to 10m winds. They also found squared correlation coefficients of about 0.70 and a root-mean-square error of 0.04 m/s. Lower turning angles and higher scaling factors would be expected off Labrador because of the lower ice thicknesses.

Table 5. Comparison of daily mean ice velocity and 10m winds (a) from the CMC regional model at the mooring site, and (b) measured at the EC meteorological station at Cartwright Labrador. using the complex regression model:

$u_i = A e^{-i\theta} u_w + C + \varepsilon$, where u_i is the ice velocity, u_w is the wind velocity, A is the scaling factor, θ is the turning angle, C is the mean ocean current, and ε is the error.

	CMC Winds				Cartwright Winds			
	2003	2005	2007	2009	2003	2005	2007	2009
Var(u_i) (m^2/s^2)	0.0518	0.0549	0.0353	0.0312	0.0518	0.0549	0.0353	0.0312
Var(u_w) (m^2/s^2)	50	47	49	54	23	21	23	25
Scaling factor(%)	2.73	2.87	2.11	1.80	3.09	3.42	2.46	2.10
Turning angle(°)	17	20	41	37	22	15	48	46
R-squared	0.72	0.70	0.61	0.56	0.42	0.45	0.40	0.36
RMS(ε) (m/s)	0.12	0.13	0.12	0.12	0.17	0.17	0.15	0.14
Current (m/s)	-0.023, 0.025	0.010, 0.007	0.018, -0.017	0.037,- 0.026	0.019, -0.003	0.022,- 0.004	0.027, -0.020	0.047,- 0.050
Days	129	99	133	124	129	99	133	124

Table 5 also shows a comparison between ice velocities and wind measured by Environment Canada at the Cartwright meteorological station. The scaling factors were 13-19% higher than for the model winds, since the model is known to overestimate surface wind speeds by 10-40% (Greenan and Prinsenberg, 1998). The turning angle was consistent with the results from the model winds. However the squared correlation coefficients are much lower (0.36-0.45) than for the

model winds (0.56-0.70), presumably because of the distance from the mooring, and topographic effects.

7.0 WIND EFFECTS ON ICE DRAFT

In the ice draft distribution plot for 2003 (Fig. 4a), there are several periods when ice thicknesses suddenly dropped to less than 0.3m (mid-March, late March and late April). These correspond to periods of offshore winds, when the thick pack ice was blown offshore and replaced with thin, newly formed ice.

In 2005, open water appeared in mid-March for about a week (Fig. 4b), following a period of onshore winds and ice drift (Fig. 9), when the ice was compressed against the coast, and the ice edge shifted inshore of the mooring site. The ice thickness changed from about 1m before the wind event, to about 4m after the wind event, when the ice was blown offshore again and probably represented rubble. Immediately following the open water period, the ice was about 1.5m for a short period, and probably represented less compressed ice near the ice edge.

In 2007, ice disappeared in the last half of February (Fig. 4c), following a period of onshore winds when the ice was compressed against the coast. The ice reappeared in late February, following a period of northerly winds, and was in the form of uniformly thick 3m ice, which probably represented rubble formed during the onshore wind event. There was a period in late March when most of the ice was less than 0.5m for several days, and which corresponded to a period of offshore winds and ice drift.

In 2009, thin ice (<0.3m draft) was present in late January during a period of offshore winds and ice drift. Several episodes of offshore winds and drift in mid-March to early April also corresponded to periods when some thin ice was present. Thin ice was absent in mid-April during a period of strong onshore winds and ice drift.

In 2011, ice disappeared for two periods in mid-February and late March respectively when there were strong onshore winds.

8.0 WATER BOTTOM TEMPERATURES

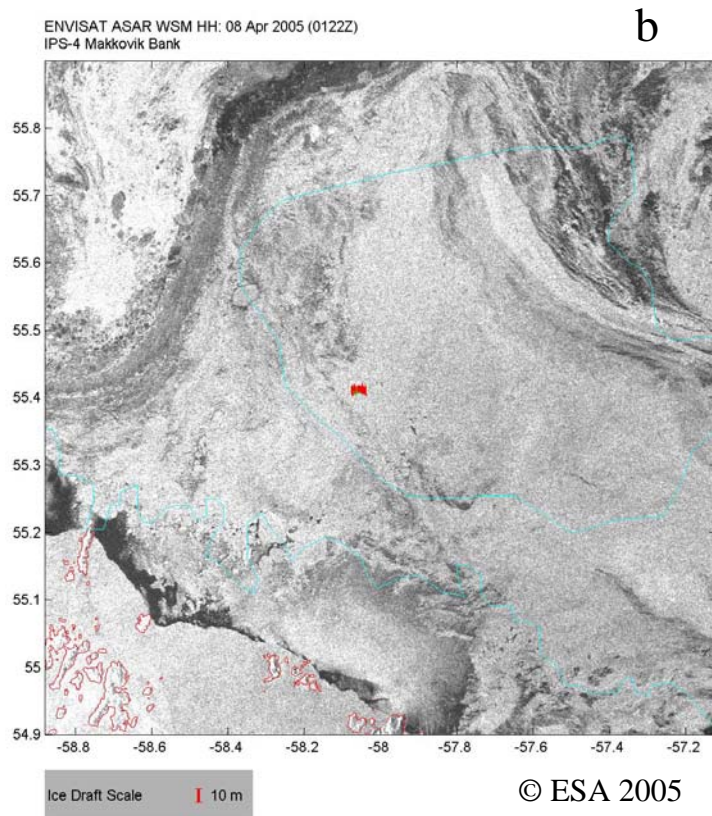
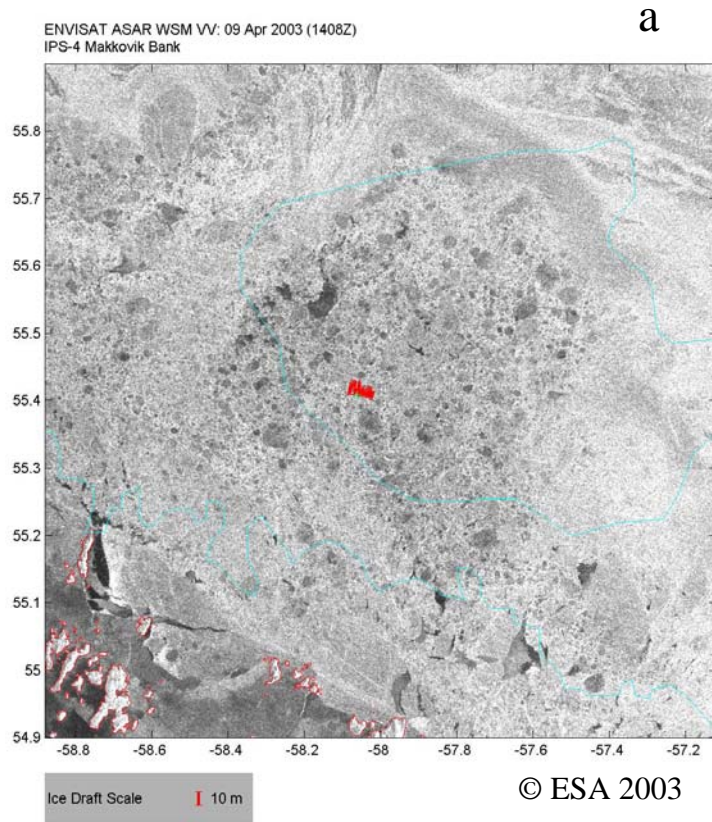
In Figure 5, water temperature measured beneath the ULS mooring with the MicroCAT recorder is plotted, along with winds and air temperature from the CMC regional model. In 2003, the bottom temperature remained near freezing from mid February to early June when the mooring was recovered. In 2005, it was near freezing for short periods between early January and mid April. In 2007, it was near freezing from mid-February to early June. In 2009, it was near freezing from mid-January to late May. In 2011, it was near freezing from mid-February to mid-May. These dates are in general agreement with when ice was present at the mooring site.

9.0 ENVISAT AND RADARSAT-2 SAR DATA

Envisat and RADARSAT-2 SAR (synthetic aperture radar) images of ice in the vicinity of the mooring site are shown in Fig. 10 (110km x 110 km) and Fig. 11 (11 km x 11 km). Envisat images are shown for 2003-2007 and RADARSAT images for 2009-2011. All images are from mid-April when ice draft is near its seasonal maximum.

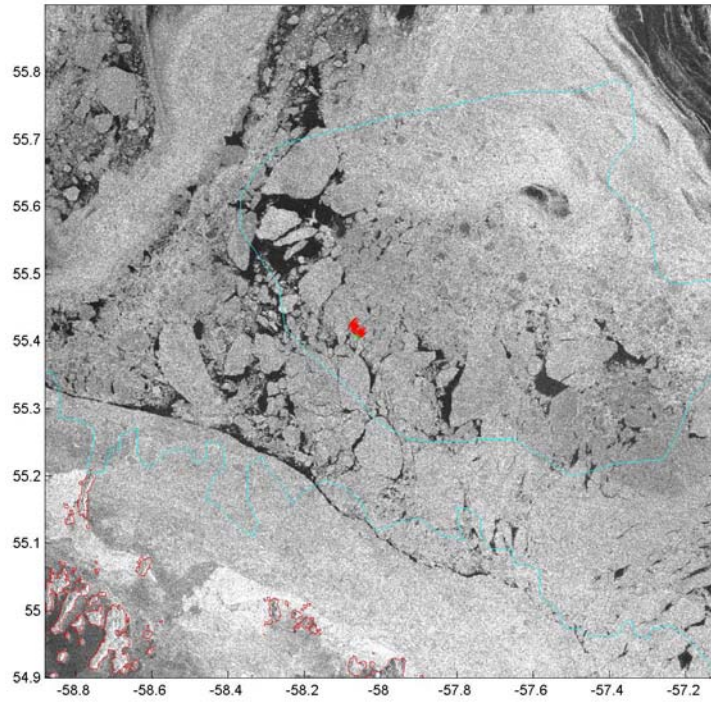
The SAR polarization is VV for 2003, and is HH for all other years. Ice draft measurements at the time of the image ± 3.6 hours are superimposed on the image as a red line. Since ice velocity measurements were not available in 2011, an ice velocity of 0.3 m/s toward the southwest was assumed for the purpose of general display. The long trajectory for 2009 indicates higher velocities than for other years. For all years except 2009, a northeastward flow through Hopedale Saddle north of Makkovik Bank is visible in the large-scale images (Fig. 10), also indicative of higher wind-driven ice drift for the 2009 image. For the 2009 image (Fig. 10d), waves can be seen propagating into the ice pack along the ice edge. A couple of bright streaks on the northwest corner of Makkovik Bank probably represent ice rubble trails downstream of grounded icebergs. The rubble would have formed as ice is driven past the icebergs by strong winds.

Figure 12 shows the ice draft histograms for the data plotted in Figs. 10 and 11. For 2003, there is a modal ice draft of about 1.2m (medium to thick first-year ice) as well as large quantities of thicker ice, probably representing deformed ice. In the SAR image (Fig. 11a), the lower drafts representing undeformed ice correspond to areas of low backscatter as expected, generally in the form of large floes. For 2005, there are ice draft modes at 0.4m (thin FY ice) and 3m (deformed ice). In the SAR image (Fig. 11b), the backscatter is high and relatively homogeneous, indicating that the ice is in the form of rubble. For 2007, there are modal ice draft of 0-0.1m (open water or new ice) and 1.4m (thick first year ice). In the SAR image (Fig. 11c) many leads (low backscatter) are visible. For 2009, the modal ice thickness is 2m (thick FY ice), and large quantities of deformed ice are present. In the SAR image (Fig. 11d), the backscatter is relatively homogeneous, with no large undeformed floes visible, in agreement with the ice draft data. For 2011, the modal ice draft is 0.6m (thin FY ice). In the SAR image (Fig. 11e), there is a large proportion of open water (low backscatter), in agreement with the ice draft data, and waves can be seen propagating through the ice.



ENVISAT ASAR WSM HH: 18 Apr 2007 (1409Z)
IPS-4 Makkovik Bank

C

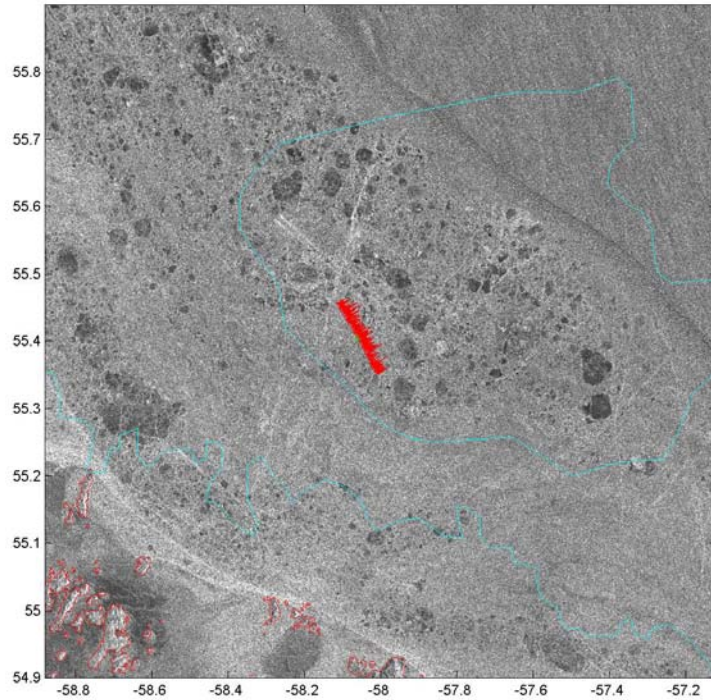


Ice Draft Scale | 10 m

© ESA 2007

RSAT2 SAR SCWA HH: 16 Apr 2009 (0959Z)
IPS-4 Makkovik Bank

d



Ice Draft Scale | 10 m

RADARSAT-2 Data and Products (c) MacDonald,
Dettwiler and Associates Ltd., 2009 - All Rights Reserved

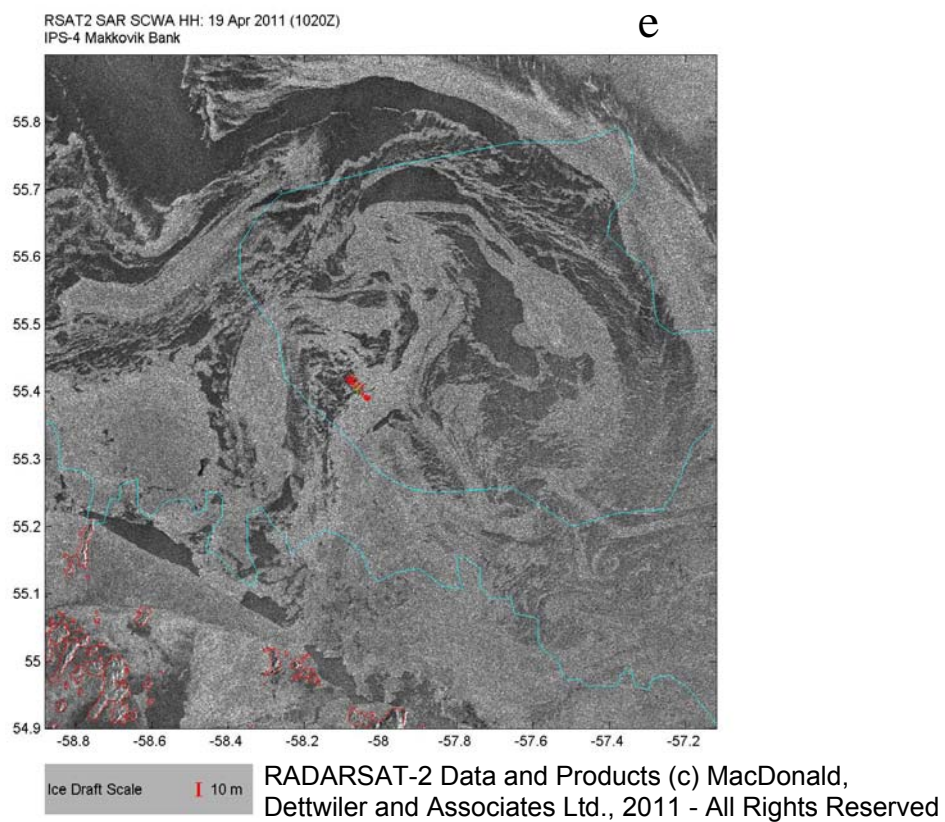
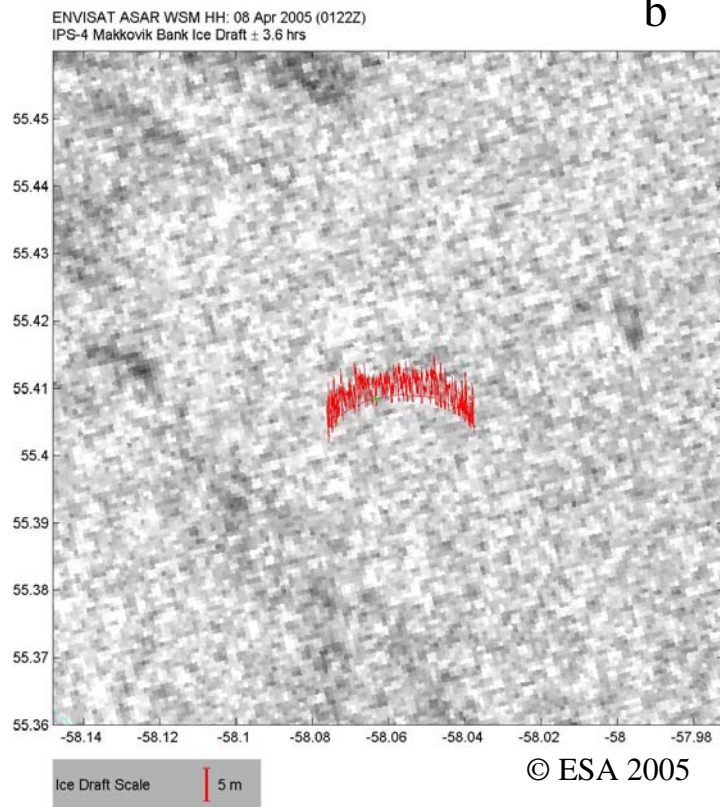
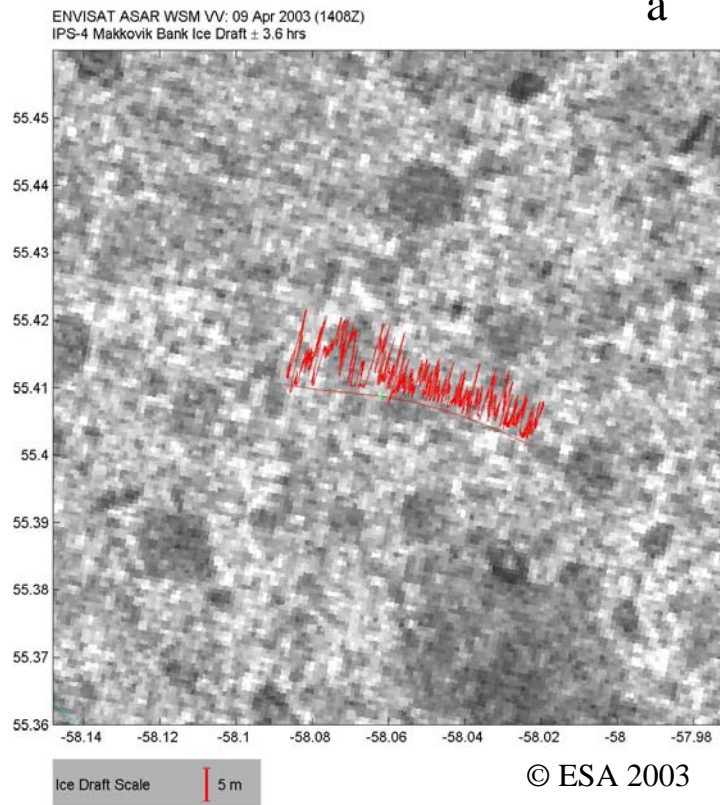
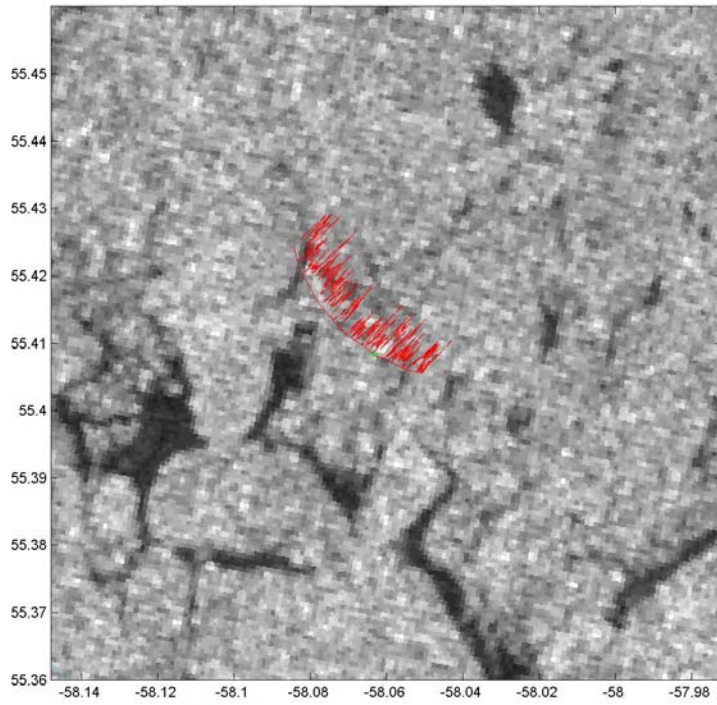


Figure 10. Envisat and RADARSAT-2 SAR images (110km x 110 km).



ENVISAT ASAR WSM HH: 18 Apr 2007 (1409Z)
IPS-4 Makkovik Bank Ice Draft \pm 3.6 hrs

c

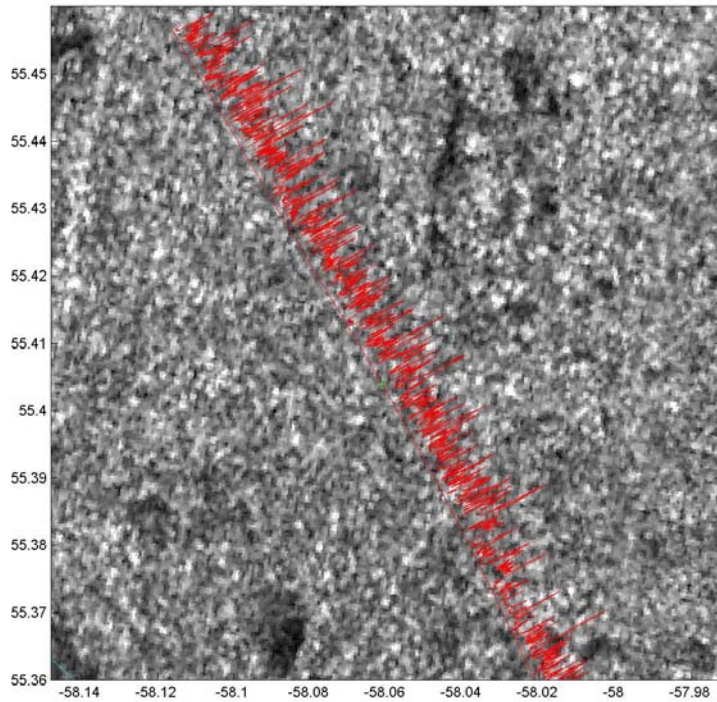


Ice Draft Scale | 5 m

© ESA 2007

RSAT2 SAR SCWA HH: 16 Apr 2009 (0959Z)
IPS-4 Makkovik Bank

d



Ice Draft Scale | 5 m

RADARSAT-2 Data and Products (c) MacDonald,
Dettwiler and Associates Ltd., 2009 - All Rights Reserved

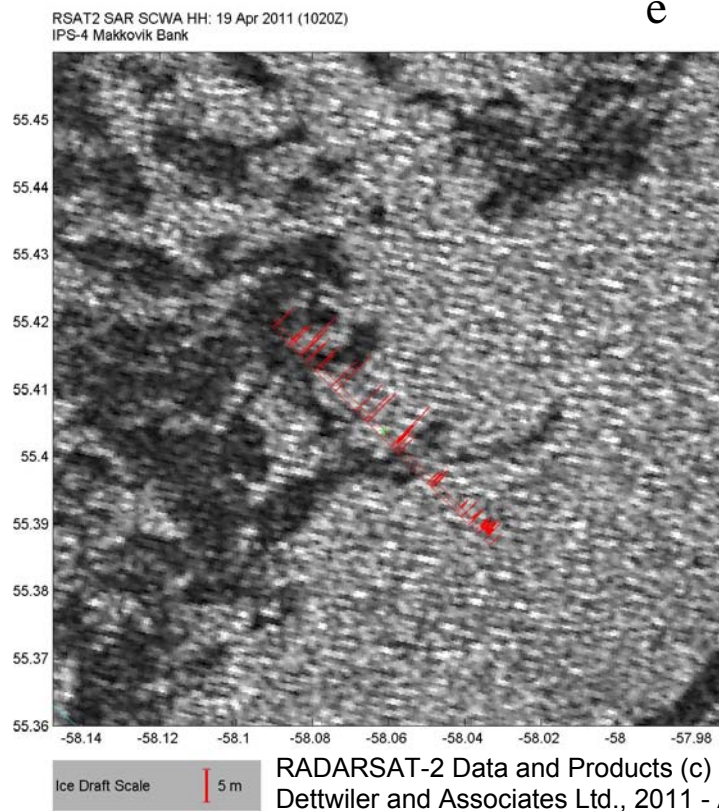


Figure 11. Envisat SAR images (11km x 11 km).

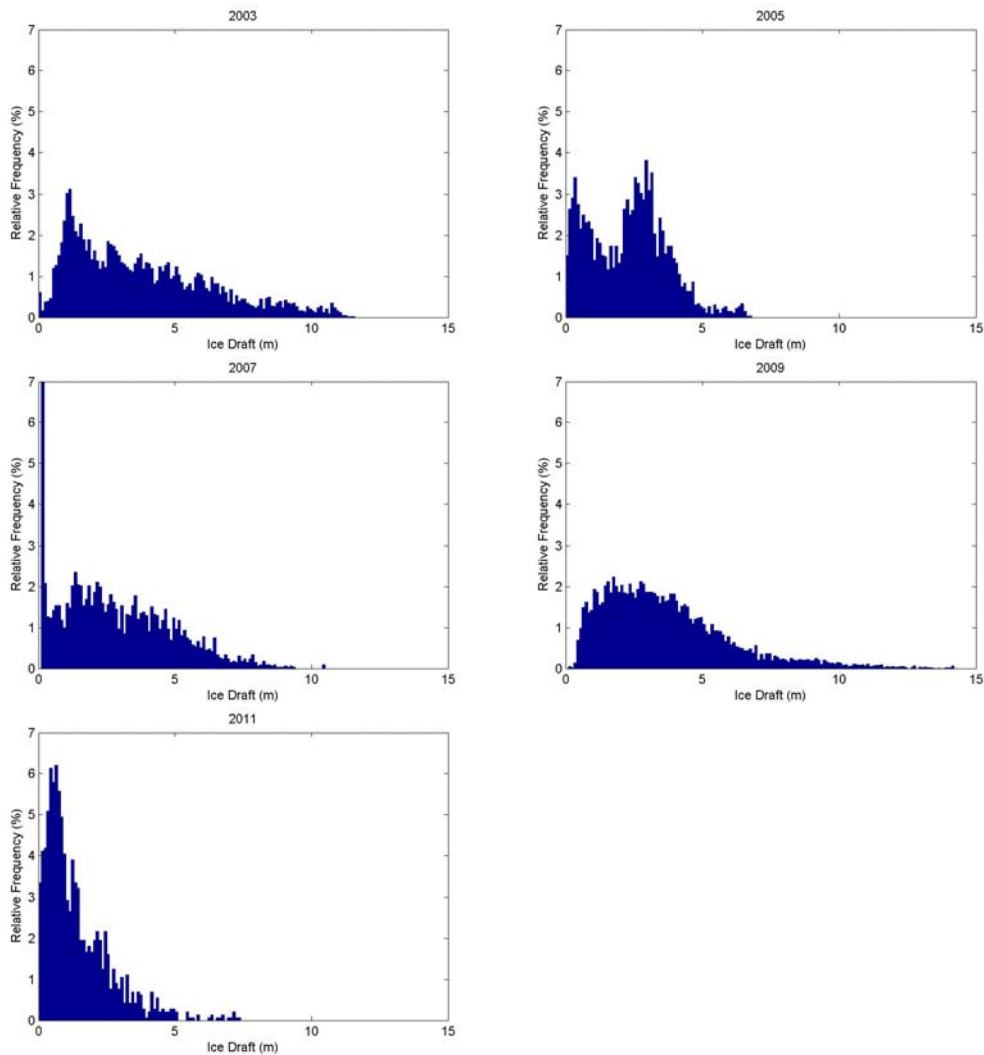


Fig. 12. Ice draft histograms for data in Figures 10 and 11.

10.0 CONCLUSIONS

- 1) The maximum ice drafts were 22, 16, 21, 21 and 21m, and the mean daily ice drafts were 2.2, 1.3, 2.8, 2.5 and 1.1m in 2003, 2005, 2007, 2009 and 2011 respectively. Periods of open water were observed when the ice was blown inshore of the mooring site. These periods were often followed by periods of very thick rubble or deformed ice, when the ice that was compressed against the shore, drifted over the mooring again. Periods of low ice thickness often corresponded to periods of offshore winds. The low mean ice thickness in 2005 was probably due to a shortage of strong northwesterly wind events so that less thick ice would be advected from the north. The low ice thickness in 2011 was probably due to fewer freezing-degree days in the early winter.

- 2) In the three heavy ice years (2003, 2007 and 2009), there appeared to be a breakdown of the deformed ice close to the onset of the melt season, when the air temperature rose above 0°C.
- 3) Ice volume inferred from the ice draft data is about twice the volume estimated from Canadian Ice Service ice charts.
- 4) Daily mean ice velocities were about 1.8-2.9% of the surface (10m) wind speed, 17-41 degrees to the right of the wind, and the wind explained 56-72% of the variance in daily mean ice velocity.
- 5) Envisat SAR data were consistent with the ice draft data. In an example from 2003, large level floes were observed in both the SAR and ice draft data. In an example from 2007, large deformed floes and many leads were observed in the data. Examples from other years showed a predominance of small floes.

11.0 ACKNOWLEDGMENTS

We wish to thank personnel from the Bedford Institute of Oceanography and the Canadian Coast Guard who assisted in the deployment and recovery of instruments, and personnel from ASL Environmental Sciences Inc. for processing the data. We also thank Tineke van der Baaren for acquiring the CMC regional model data. This work was supported by the Canadian Panel on Energy Research and Development (PERD) and the Canadian Space Agency Government-Related Initiatives Program (GRIP). ENVISAT ASAR data were provided by the European Space Agency under AO Project 178. NCEP Reanalysis data was provided by the NOAA/OAR/ESRL PSD, Boulder, Colorado, USA, from their Web site at <http://www.esrl.noaa.gov/psd/>.

12.0 REFERENCES

Environment Canada. 2005. Manual of Standard Procedures for Observing and Reporting Ice Conditions (MANICE). Issuing authority: Assistant Deputy Minister, Meteorological Service of Canada: <http://www.ec.gc.ca/glaces-ice/default.asp?lang=En&n=08D7D137-1>.

Greenan, B.J.W. and S. Prinsenberg, 1998. Wind forcing of ice cover in the Labrador Shelf marginal ice zone, *Atmosphere-Ocean* 36:71-93.

Hamilton, J., S. Prinsenberg, and L. Malloch. 2002. Moored current meter and CTD observations from Barrow Strait, 1998-1999. *Can. Data Rep. Hydrogr. Ocean Sci.* 157: v + 65 pp.

Kalnay et al. (1996), The NCEP/NCAR 40-year reanalysis project, *Bull. Amer. Meteor. Soc.*, 77: 437-470

LeBlond, P.H. 1982. Satellite observations of Labrador current undulations. *Atmosphere-Ocean* 20(2): 129-142.

- Marchenko, A. 2008. Thermodynamic consolidation and melting of sea ice ridges, *Cold Regions Science and Technology* 52: 278–301.
- Melling, H. and D.A. Riedel, 1996. Development of seasonal pack ice in the Beaufort Sea during the winter of 1991-1992: A view from below. *Journal of Geophysical Research* 101(C5): 11975-11991.
- Melling, H. and Riedel, D.A.. 2004. Draft and Movement of Pack Ice in the Beaufort Sea: A Time-Series Presentation, April 1990 – August 1999. Can. Tech. Rep. Hydrogr. Ocean Sci. No. 238. v + 24 p.
- Prinsenber, S.J., I.K. Peterson, J.S. Holladay and L. Lalumiere, 2011. Labrador Shelf Pack Ice and Iceberg Survey, March 2009. Can Tech. Rep. Hydrogr. Ocean Sci. 269: viii+76p.
- Prinsenber, S.J., I.K. Peterson, J.S. Holladay and L. Lalumiere, 2012. Labrador Shelf Pack Ice and Iceberg Survey, March 2011. Can. Tech. Rep. Hydrogr. Ocean Sci. 275: vii+44pp.
- Ross, E.I, K. Borg and D.B. Fissel, 2006. Data Processing and Analysis of Ice Keel Depths and Ice Velocities, Makkovik Bank, 2002-2003 and 2004-2006. Report for the Bedford Institute of Oceanography, Dartmouth, NS Canada by ASL Environmental Sciences Inc, Sidney, B.C. Canada vi + 45 p + unnumbered appendices
- Steer, A. D., Worby, A.P., Heil, P. 2008. Observed changes in sea-ice floe size distribution during early summer in the western Weddell Sea. *Deep-Sea Research II* 55 (8-9): 933-942.
- Thorndike, A. S., and R. Colony (1982), Sea Ice Motion in Response to Geostrophic Winds, *J. Geophys. Res.*, 87(C8), 5845–5852, doi:10.1029/JC087iC08p05845.
- Wadhams, P., McLaren, A., S., and Weintraub, R. (1985) Ice thickness in Davis Strait in February from submarine sonar profiles. *Journal of Geophysical Research* 90: 1069-1077.